BH_2^+, mass 13. Since we determined by velocity analysis that 32% of mass 13 was due to a BH_3 precursor, then 2.7% of the total material leaving the pyrolyzer is BH_3 appearing as mass 13. Mappes and Fehlner's[18] determination of the electron bombardment fragmentation pattern for BH_3 gave 56.4% as mass 13. Dividing 2.7% by this fragmentation factor leads to a total of 4.8% BH_3 production. Since the assumed mechanism is $B_2H_6 \rightarrow 2BH_3$, 2.4% of the B_2H_6 is decomposing to molecular borane at our experimental conditions. This result may be compared to that of Fehlner and Fridman,[10] who reported a maximum BH_3 yield of 0.8% at 650 K.

We have now provided unambiguous evidence for the production of borane from pyrolyzed diborane. It is also evident that the experimental technique which has been developed here has expanded the utility of the mass spectrometer for determining thermodecomposition mechanisms in the gas phase.

Acknowledgment. We thank NASA (Grant No. NGL 01-008-001) and The University of Alabama in Huntsville Research Committee for their support.

Registry No. B_2H_6, 19287-45-7; BH_3, 13283-31-3.

References and Notes

(1) This research constitutes partial fulfillment of the M.S. degree requirements of B.S.A.
(2) W. N. Lipscomb, "Boron Hydrides", W. A. Benjamin, New York, N.Y., 1970.
(3) L. H. Long, *Prog. Inorg. Chem.*, **15** (1972).
(4) H. R. Bachmann, H. Nöth, R. Rinck, and K. L. Kompa, *Chem. Phys. Lett.*, **29**, 627 (1974).
(5) H. R. Bachmann, H. Nöth, R. Rinck, and K. L. Kompa, *Chem. Phys. Lett.*, **33**, 261 (1975).
(6) R. P. Clarke and R. N. Pease, *J. Am. Chem. Soc.*, 73, 2132 (1951).
(7) J. K. Bragg, L. V. McCarty, and F. J. Norton, *J. Am. Chem. Soc.*, **73**, 2134 (1951).
(8) T. P. Fehlner and W. S. Koski, *J. Am. Chem. Soc.*, **86**, 2733 (1964).
(9) T. P. Fehlner, *J. Am. Chem. Soc.*, **87**, 4200 (1965).
(10) T. P. Fehlner and S. A. Fridman, *Inorg. Chem.*, **9**, 2288 (1970).
(11) E. J. Sinke, G. A. Pressley, Jr., A. B. Baylis, and F. E. Stafford, *J. Chem. Phys.*, **41**, 2207 (1967).
(12) J. H. Wilson and H. A. McGee, Jr., *J. Chem. Phys.*, **46**, 1444 (1967).
(13) A. Cornu and R. Massot, "Compilation of Mass Spectral Data Index De Spectres De Masse", Heyen and Son, London, 1966.
(14) A. E. Grosser, *Rev. Sci. Instrum.*, **38**, 257 (1967).
(15) The velocity selector was driven by a Globe Inc. hysteresis synchronous motor, Type FC. The motor was powered by a frequency generator, variable-capacitance unit, and Dynakit stereoamplifiers series network.
(16) $I(V) \propto V^3 e^{-MV^2/2RT}$.
(17) Extranuclear Laboratories, Inc., custom 5-in. quadrupole, high-efficiency ionizer and off-axis solid-state multiplier.
(18) G. W. Mappes and T. P. Fehlner, *J. Am. Chem. Soc.*, **92**, 1562 (1970).

Contribution from the Department of Chemistry,
University of North Carolina, Chapel Hill,
North Carolina 27514

On the Superexchange Mechanism in Polymeric Heterocyclic Diamine Bridged Copper(II) Complexes. 2

H. Wayne Richardson, John R. Wasson,
and William E. Hatfield*

Received July 26, 1976 AIC60540E

Within recent years numerous studies of metal complexes of pyrazine (pyr) have been described.[1-6] In spite of its low basicity ($pK_{a_1} = 0.65$[7]) pyrazine can function as a bridging bidentate ligand giving rise to dimers, e.g., $[(NH_3)_5Ru^{II}$–pyr–$Ru^{III}(NH_3)_5]^{5+}$,[5] and polymers, e.g., $[Cu(hfac)_2 \cdot pyr]_n$.[4] Previously, we have examined $[Cu(NO_3)_2 \cdot pyr]_n$[1-3] and related compounds[8-10] by magnetic susceptibility techniques and have shown conclusively that antiferromagnetic spin coupling is affected by way of the π system of the heterocyclic ligand. Also, Creutz and Taube[5] have observed spectroscopically an intervalence-transfer band in the mixed-valence compound $[(NH_3)_5Ru^{II}$–pyr–$Ru^{III}(NH_3)_5]^{5+}$. The fact that the π system of pyrazine provides an excellent pathway for spin–spin interactions between metal ions is well documented. It was of interest to determine the nature of the spin–spin interactions, if any, across the pyrazine bridge in $Cu(hfac)_2 \cdot pyr$ and to compare the results with $Cu(hfac)_2 \cdot$Dabco (Dabco = 1,4-diazabicyclo[2.2.2]octane). In the latter compound the interaction can occur only by a σ-bond mechanism. To supplement this work, the 1,5-naphthyridine complex of $Cu(hfac)_2$ was prepared and studied. The results of these studies are reported herein.

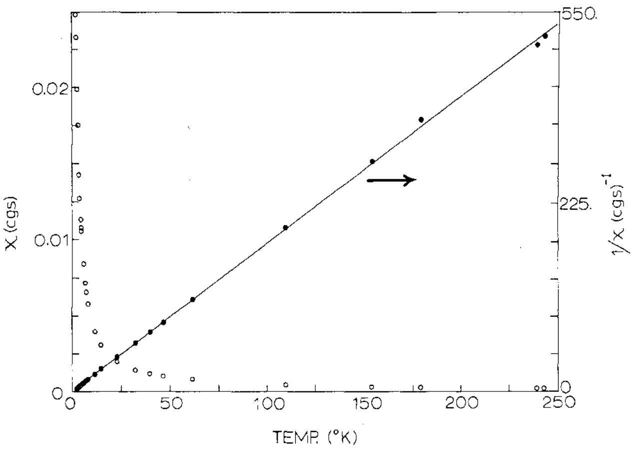

Figure 1. Magnetic susceptibility data (○) and reciprocal magnetic susceptibility (•) for the $Cu(hfac)_2 \cdot pyr$ complex from 1.8 to 250 K. The solid line is the best fit of the data to the Curie–Weiss equation.

Experimental Section

All of the complexes were prepared by adding stoichiometric (1:1) amounts of ligand in tetrachloromethane to diaquobis(1,1,1,5,5,5-hexafluoropentane-2,4-dionato)copper(II), $[Cu(hfac)_2(H_2O)_2]$.[4,11] The precipitated complexes, $[Cu(hfac)_2L]_n$, were washed with tetrachloromethane and air-dried. Anal.[12] Calcd for $Cu(hfac)_2 \cdot pyr$, $C_{14}H_6N_2O_4F_{12}Cu$: C, 30.15; H, 1.08; Cu, 11.4. Found: C, 29.92; H, 1.07; Cu, 11.6. Calcd for $Cu(hfac)_2 \cdot$Dabco, $C_{16}H_{14}N_2O_4F_{12}Cu$: C, 32.58; H, 2.39; Cu, 10.8. Found: C, 32.48; H, 2.30; Cu, 10.7. Calcd for $Cu(hfac)_2 \cdot$1,5-naphthyridine, $C_{18}H_8N_2O_4F_{12}Cu$: C, 35.58; H, 1.33; Cu, 10.4. Found: C, 35.28; H, 1.21; Cu, 10.6. Copper was determined by EDTA titration with SNAZOX indicator.[13] 1,5-Naphthyridine was prepared as described previously.[14]

Magnetic susceptibilities were determined with a Foner-type vibrating-sample magnetometer[15] operating at a field strength of 10000 G. Calibration of the magnetometer was checked using $HgCo(NCS)_4$[16] with the more recent correction to the Weiss constant[17] being applied and then recalibrated with $(NH_4)_2Mn(SO_4)_2 \cdot 6H_2O$.[18] Both standards agreed within 2%. The magnetic field was calibrated as previously reported[19] and is accurate to better than 0.15% at 10 kG. Sample temperature was measured with a gallium arsenide diode that had been standardized against a commercially calibrated diode.[20] A value of 60×10^{-6} cgsu was used for the temperature-independent paramagnetism of the copper(II) ion and constituent diamagnetic corrections were estimated from Pascal's constants.[21] The EPR spectra were taken with a Varian E-3 X-band spectrometer. The magnetic field, klystron frequency, and field sweep were checked using the double standard: DPPH free radical ($g = 2.0036$) and vanadyl(IV) acetylacetonate in benzene.[22] Electronic spectra were obtained on a Cary 17 recording spectrophotometer using a mull (transmission) technique described previously.[23]

Results

The magnetic susceptibility data for the $Cu(hfac)_2 \cdot pyr$ complex are shown as a function of temperature in Figure 1. The behavior of all three complexes is similar; the data are typical of spin $^1/_2$ paramagnets[24] and obey the Curie–Weiss

Table I. Spectroscopic and Magnetic Data for the $Cu(hfac)_2\cdot L$ Complexes

Complex	Visible spectra, μm^{-1}	EPR data			Magnetic susceptibility parameters		
		$g_\parallel$ (±0.005)	$g_\perp$ (±0.005)	$\langle g \rangle$	$\langle g \rangle$	Θ, deg	P
$Cu(hfac)_2\cdot pyr$	(1.39)[a] 1.47	2.246	2.114	2.158	2.24 ± 0.01	−0.54 ± 0.5	9.02
$Cu(hfac)_2\cdot nap$	(1.39) 1.47	2.282	2.100	2.161	2.19 ± 0.01	0.04 ± 0.3	1.74
$Cu(hfac)_2\cdot Dabco$	(1.37) 1.46	2.251	2.112	2.158	2.22 ± 0.01	−0.21 ± 0.2	0.23

[a] Shoulder.

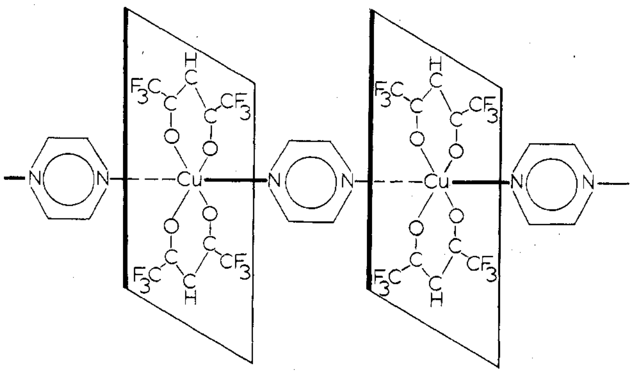

Figure 2. Linear-chain structure for $Cu(hfac)_2\cdot pyr$.

law given by $\chi = [Ng^2\beta^2/3k(T - \Theta)][S(S + 1)]$.[25] The magnetic g values and Weiss constants, Θ, were calculated by standard linear least-squares methods where the best fits were obtained by using the minimum value of

$$P = \sum_{i=1}^{n} [1/\chi_o - 1/\chi_c]^2/n$$

which is linear in temperature, as the criterion for the best fit. The magnitudes of the Θ values are indicative of small interactions present between the copper ions.

The electronic spectra of all three complexes are very similar. The spectrum of the pyrazine complex exhibits a d–d band maximum near 1.47 μm^{-1} while the band maximum of the $Cu(NO_3)_2\cdot pyr$ complex[3] is near 1.75 μm^{-1}. The structural implications are presented below. The electronic spectral data of all of the $Cu(hfac)_2\cdot L$ complexes are given in Table I.

The electron paramagnetic resonance (EPR) spectra of polycrystalline samples of all of the complexes are characteristic of a tetragonal geometry. No hyperfine structure was resolved; only two g values, $g_\parallel$ and $g_\perp$, were observed and these are reported in Table I.

Discussion

The linear-chain structure of $Cu(hfac)_2\cdot pyr$[4] is qualitatively depicted in Figure 2. The structure of $Cu(hfac)_2\cdot Dabco$[11] is very similar. The environment about the copper(II) ion for the $Cu(hfac)_2\cdot pyr$ complex (Figure 3a) consists of four short (~1.96 Å) in-plane bonds to the oxygen atoms of the two hfac ligands and two longer (2.53 Å) out-of-plane bonds to the pyrazine nitrogens giving rise to the usual "4 + 2" tetragonal configuration. The magnetic and spectroscopic data support the same configuration for the $Cu(hfac)_2\cdot nap$ complex (nap = naphthyridine). The environment about the copper(II) ion in $Cu(NO_3)_2\cdot pyr$[26] is considerably different as shown in Figure 3b. In this case the pyrazine nitrogens are bound in plane (1.98 Å), with the nitrate ions bound with two short (2.01 Å) copper–oxygen in-plane bonds and two long (2.49 Å) out-of-plane bonds completing the highly distorted six-coordinated geometry.

If the postulated mechanism for spin coupling in $Cu(NO_3)_2\cdot pyr$[3] is viewed, certain assessments can be made in regard to the absence of observable spin coupling in the $Cu(hfac)_2\cdot L$ systems. Magnetic exchange in the $Cu(NO_3)_2\cdot pyr$ complex is brought about by virtue of overlap between the

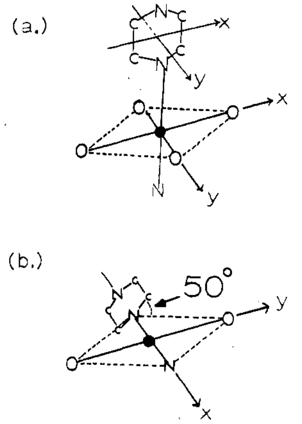

Figure 3. Environment about the copper(II) ion in (a) $Cu(hfac)_2\cdot pyr$ and (b) $Cu(NO_3)_2\cdot pyr$. The relative positions of the pyrazine ring plane in each structure are indicated.

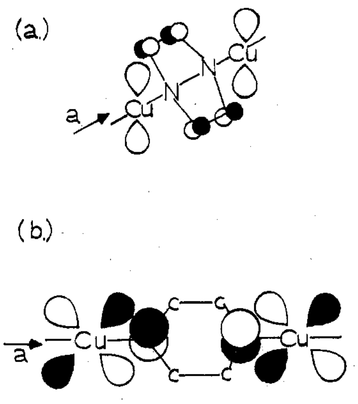

Figure 4. Symmetry-allowed possibilities for d–π overlap in $Cu(NO_3)_2\cdot pyr$: (a) $d_{x^2-y^2}$–π(b_{1g}); (b) d_{xy}–π(b_{2g}). The x axis of Figure 3b is taken to be collinear with the a axis indicated on the figure.

copper d orbitals and the pyrazine π system.[3] Using symmetry arguments it may be readily seen that two possibilities for d–π overlap are allowed.

The pyrazine groups lie canted some 50° out of the copper xy plane and this allows for $d_{x^2-y^2}$–π(b_{1g}) overlap as shown in Figure 4a.. The unpaired electron is predominantly in the $d_{x^2-y^2}$ orbital[27] which overlaps with the highest occupied molecular π orbital of pyrazine (b_{1g})[28] giving rise to one

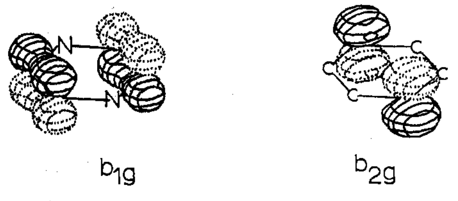

pathway for superexchange. Alternately, the possibility for overlap of the $d_{xy,xz}$–π(b_{2g}) orbitals is shown in Figure 4b. Ab initio SCF–CI methods[28] have shown the b_{2g} orbital in pyrazine to lie some 300 cm^{-1} lower in energy than the HOMO (b_{1g}). Even though a more direct overlap is afforded with the $d_{xy,xz}$–π(b_{2g}) orbitals than with the $d_{x^2-y^2}$–π(b_{1g}) orbitals, the resulting antiferromagnetic alignment of unpaired spins from $d_{xy,xz}$–π–$d_{xy,xz}$ overlap must arise from secondary factors. Some unpaired spin density will be incorporated in the d_{xy} orbital allowing for a d_{xy}–$\pi(b_{2g})$–d_{xy} superexchange pathway.

In the $Cu(hfac)_2$·pyr complex the plane of the pyrazine ligands lies in the *xz* plane of the $Cu(hfac)_2$ unit.[4] The site symmetry about the copper(II) ion is C_{2h}. If superexchange is to occur by a π pathway, we need only consider overlap of the $d_{x^2-y^2}$, d_{xy}, and d_{z^2} orbitals of copper with the π system of pyrazine since under C_{2h} symmetry these are the only metal orbitals with unpaired spin density. The only symmetry-allowed overlap with the pyrazine π system arises from d_{xy}–$\pi(b_{1g})$ overlap corresponding to the $d_{x^2-y^2}$–$\pi(b_{1g})$ overlap in $Cu(NO_3)_2$·pyr (Figure 4a). However, in $Cu(hfac)_2$·pyr we have the combination of the small amount of unpaired spin density in d_{xy} and poor effective overlap as obtains from d–$\pi(b_{1g})$ orbitals. A superexchange interaction in $Cu(hfac)_2$·pyr was not observed within the limits of our experiments (1.8 K) even though a π pathway is available.

The magnetic susceptibility data as a function of temperature for the $Cu(hfac)_2$·Dabco complex do not reveal magnetic-exchange interactions. The only tenable pathway for superexchange along the chain is by way of σ orbitals, since Dabco is without a π system; however, exchange along a σ pathway would be severely attenuated over the long Cu–Cu separation of 7.7 Å.[11] Also, the metal orbital that overlaps with the σ system of the Dabco is mainly of d_{z^2} character, and this orbital has little unpaired spin density.

The $Cu(NO_3)_2$·nap complex[9] has been studied previously by magnetic susceptibility methods and found to exhibit enhanced spin coupling relative to the $Cu(NO_3)_2$·pyr complex in spite of the larger Cu–Cu separation (~9 Å vs. 6.7 Å). The enhanced spin coupling relative to pyrazine is a consequence of the nature of the π system of the 1,5-naphthyridine. Our initial interest in studying the complex $Cu(hfac)_2$·nap was stimulated by the greater basicity of 1,5-naphthyridine. We attempted to prepare a $Cu(hfac)_2$ complex with in-plane copper–nitrogen bonds analogous to *cis*-$Cu(hfac)_2$·2py.[29] We conjectured the possibility that the stability of the in-plane pyridine arrangement was due to the greater basicity of the pyridine ligand ($pK_a \approx 5.2$) as compared to that of pyrazine. A cis or trans arrangement for the $Cu(hfac)_2$·nap should have given rise to dimeric or polymeric structures, respectively, and the expected shorter (in-plane) copper–ligand bond should have been more conducive to magnetic-exchange interactions. The electronic, EPR, and magnetic data (see Table I) for the $Cu(hfac)_2$·nap complex are virtually analogous to the data for $Cu(hfac)_2$·pyr and $Cu(hfac)_2$·Dabco, and we conclude that its structure is similar.

Acknowledgment. This research was supported by the National Science Foundation under Grant No. MPS74-11495 and by the Materials Research Center of the University of North Carolina under Grant No. DMR72-03024 from the National Science Foundation.

Registry No. $Cu(hfac)_2$·pyr, 52151-41-4; $Cu(hfac)_2$·nap, 61075-79-4; $Cu(hfac)_2$·Dabco, 38548-37-7.

References and Notes

(1) J. F. Villa and W. E. Hatfield, *J. Am. Chem. Soc.*, **93**, 4081 (1971).
(2) D. B. Losee, H. W. Richardson, and W. E. Hatfield, *J. Chem. Phys.*, **59**, 3600 (1973).
(3) H. W. Richardson and W. E. Hatfield, *J. Am. Chem. Soc.*, **98**, 835 (1976).
(4) R. C. E. Belford, D. E. Fenton, and M. R. Truter, *J. Chem. Soc., Dalton Trans.*, 17 (1974).
(5) C. Creutz and H. Taube, *J. Am. Chem. Soc.*, **95**, 1006 (1973).
(6) R. W. Callahan, G. M. Brown, and T. J. Meyer, *Inorg. Chem.*, **14**, 1443 (1975).
(7) A. Chia and R. F. Trimble, Jr., *J. Phys. Chem.*, **65**, 863 (1961).
(8) H. W. Richardson, W. E. Hatfield, H. J. Stoklosa, and J. R. Wasson, *Inorg. Chem.*, **12**, 2051 (1973).
(9) H. J. Stoklosa, J. R. Wasson, E. V. Brown, H. W. Richardson, and W. E. Hatfield, *Inorg. Chem.*, **14**, 2378 (1975).
(10) H. W. Richardson, J. R. Wasson, W. E. Hatfield, E. V. Brown, and A. Plasz, *Inorg. Chem.*, **15**, 2916 (1976).
(11) R. C. E. Belford, D. E. Fenton, and M. R. Truter, *J. Chem. Soc., Dalton Trans.*, 2208 (1972).
(12) C and H analyzed by Integral Microanalytical Labs, Raleigh, N. C.
(13) G. Guerrin, M. V. Sheldon, and C. N. Reilley, *Chemist-Analyst*, **49**, 36 (1960).
(14) Y. Hamada and I. Takeuchi, *Chem. Pharm. Bull.*, **19**, 1857 (1971).
(15) S. Foner, *Rev. Sci. Instrum.*, **30**, 548 (1959).
(16) B. N. Figgis and R. S. Nyholm, *J. Chem. Soc.*, 4190 (1958).
(17) H. St. Rade, *J. Phys. Chem.*, **77**, 424 (1973).
(18) F. R. McKim and W. P. Wolf, *J. Sci. Instrum.*, **34**, 64 (1957).
(19) D. B. Losee and W. E. Hatfield, *Phys. Rev. B*, **10**, 212 (1974).
(20) Type TG-100 FPA (Special), No. 4277, Lake Shore Cryotronics, Eden, N.Y.
(21) E. Konig, "Magnetic Properties of Transition Metal Compounds", Springer-Verlag, Berlin, 1966.
(22) I. Bernal and P. H. Rieger, *Inorg. Chem.*, **2**, 256 (1963); D. H. Chen and G. R. Luckhurst, *Trans. Faraday Soc.*, **65**, 656 (1969).
(23) J. R. Wasson, *Chemist-Analyst*, **56**, 36 (1967).
(24) J. S. Smart, "Effective Field Theories of Magnetism", W. B. Saunders, Philadelphia, Pa., 1966.
(25) P. Weiss, *Radium (Paris)*, **4**, 661 (1907).
(26) A. Santoro, A. D. Mighell, and C. W. Reimann, *Acta Crystallogr., Sect. B*, **26**, 979 (1970).
(27) G. F. Kokoszka and C. W. Reimann, *J. Inorg. Nucl. Chem.*, **32**, 3229 (1970).
(28) M. Hackmeyer and J. L. Whitten, *J. Chem. Phys.*, **54**, 3739 (1971).
(29) J. Pradilla-Sorzano and J. P. Fackler, Jr., *Inorg. Chem.*, **12**, 1174 (1973).

Contribution from the Department of Chemistry,
Oklahoma State University, Stillwater, Oklahoma 74074

Coordination of Water in Alkali Metal Oxy Anion Glasses

G. Ritzhaupt and J. P. Devlin*

Received August 25, 1976 AIC60629K

There is considerable interest in the nature of the interactions experienced by water molecules within a molten salt like environment with a particular concern for the relative importance of cation–H_2O and anion–H_2O interactions.[1] Part of this interest arises because the H_2O molecule environment, which is undoubtedly quite varied in more dilute water solutions, is presumed to be more uniform since there is little chance for H_2O–H_2O interactions to further complicate the structure. However, the observation and interpretation of vibrational spectra for H_2O molecules isolated in such an environment presents some special problems, with the result that no infrared data are available for single-salt systems. In addition to the naturally great bandwidth for the H_2O stretching modes, thermal band broadening is a complicating factor at molten salt temperatures. Other discouraging factors include corrosion of cell materials, sample instability, the need for a constant appropriate H_2O vapor pressure, and the possibility of some aggregation of the H_2O molecules.

Much of the difficulty in obtaining the infrared spectra of polar molecules, such as H_2O, isolated from one another within a molten salt like environment can be avoided by isolating the molecules in a glassy salt matrix prepared by condensing the molten salt vapors at 80 K.[2] When the salt vapors are generated within a Knudsen effusion cell at temperatures near the melting point, there is no significant contamination of the glassy deposit by decomposition products for the alkali metal nitrates,[3] chlorates,[4,5] perchlorates,[6] or thiocyanates, with the exception of the lithium salt of the chlorate ion.[4]

In the present study the H_2O impurity molecules in the glassy salt matrices originated from residual water within the molten salts and/or the vacuum system after the salts were dried for 12 h at ~200 °C.[4] Thus, the precise H_2O concentrations were not known, but in each instance the ν_3